Multicenter Trial Validation for Quantitative Analysis of Same-Day Rest-Stress Technetium-99m-Sestamibi Myocardial Tomograms

Kenneth F. Van Train, Ernest V. Garcia, Jamshid Maddahi, Joseph Areeda, C. David Cooke, Hosen Kiat, Gerrard Silagan, Russell Folks, John Friedman, Lisa Matzer, Guido Germano, Tim Bateman, Jack Ziffer, E. Gordon DePuey, Darlene Fink-Bennett, Karen Cloninger and Daniel S. Berman

Departments of Imaging (Nuclear Medicine), and Medicine, (Division of Cardiology), Cedars-Sinai Medical Center; University of California School of Medicine, Los Angeles, California; Emory University School of Medicine, Atlanta, Georgia; and the Multicenter Trial Sites

The accuracy of an automated quantitative analysis of same-day rest/stress ^{99m}Tc sestamibi SPECT images for detection and localization of coronary artery disease (CAD) was assessed in a multicenter trial consisting of 161 patients from 7 different clinical sites utilizing various camera computer systems. **Methods:** Of the 161 patients, 102 had angiographically documented coronary artery disease, 22 had normal coronary arteriograms, and 37 had a low (<5%) likelihood of coronary artery disease based on their age, sex, symptoms and the results of their exercise electrocardiograms. The patients were studied using previously optimized image acquisition and processing protocols. An additional population consisting of 45 patients with single-vessel disease were evaluated to determine the optimal criteria for detection of CAD. **Results:** The quantitative analysis method was associated with an overall sensitivity of 87%, specificity of 36%, and normalcy rate (true negative rate in the low likelihood patients) of 81%. Sensitivity for overall detection of disease was similar (90%) in patients with and without myocardial infarction (90% versus 89%). The sensitivities and specificities for identification of disease in individual coronary arteries were, respectively, 69% and 76% for LAD, 70% and 80% for LCX, and 77% and 85% for RCA. **Conclusion:** The results of this study demonstrate that the new objective quantitative method for analysis of same-day rest/stress ^{99m}Tc sestamibi SPECT images is accurate for detection and localization of CAD and correlates highly with expert visual interpretation.

Key Words: multicenter trial; coronary artery disease; technetium-99m-sestamibi

J Nucl Med 1994; 35:609–618

Technetium-99m-sestamibi is a new myocardial perfusion imaging agent that has favorable imaging characteristics for myocardial perfusion imaging (*1–7*). Since its clinical introduction in 1992, rest/stress ^{99m}Tc-sestamibi myocardial perfusion imaging is increasingly being used for detection and localization of coronary artery disease (CAD). Experience with ^{201}Tl myocardial perfusion imaging has highlighted the need for quantitative approaches for the analysis of planar and tomographic images (*8–21*) in order to objectify image interpretation and to provide a more accurate means of assessing the extent, severity and reversibility of perfusion defects. Earlier quantitative methods for ^{99m}Tc sestamibi image analysis were applied to studies which were not acquired by optimized imaging protocols (*22,23*). In this refined approach, we initially optimized image acquisition and processing protocols in order to take full advantage of the superior physical and imaging characteristics of this agent (*24,25*). Furthermore, novel quantitative analysis algorithms were implemented which included automatic feature extraction (*26*), optimized myocardial sampling and comprehensive polar map analysis (*24,25*). Gender-matched normal limits were then established and objective criteria for detection and localization of CAD were developed and validated (*27*).

The present study was undertaken to assess the accuracy of the quantitative program for detection and localization of CAD and to evaluate the applicability of the method in different imaging laboratories, utilizing various computer systems and patients from differing geographical locations.

MATERIALS AND METHODS

Patient Populations

The normal limits and criteria for abnormality were developed previously (*27*). The normal population was defined as having a <5% likelihood of CAD based on sequential Bayesian analysis of age, sex, symptom classification and the results of exercise electrocardiography (*20,28,29*). The current study included an inves-

Received Aug. 6, 1993; revision accepted Dec. 9, 1993.

For correspondence or reprints contact: Kenneth F. Van Train, Cedars-Sinai Medical Center, Department of Nuclear Medicine, 8700 Beverly Blvd., Los Angeles, CA 90048.

TABLE 1
Multicenter Trial Sites and Investigators

	Location	Principal Investigator
Siemens Sites (Type A)		
Cardiac and Vascular Diag. Ctr.	Los Angeles, CA	John Friedman, MD
Cardiovascular Consultants	Kansas City, MO	Tim Bateman, MD
Northside Cardiology P.C.	Indianapolis, IN	Roland Landin, MD
GE Sites (Type B)		
Emory University	Atlanta, GA	Jack Ziffer, MD
Roosevelt/St. Luke's Hospital	New York, NY	E. Gordon DePuey, MD
William Beaumont Hospital	Detroit, MI	Darlene Fink-Bennett, MD
Central Florida Cardiology	Orlando, FL	Karen Cloninger, MD

tigation to establish criteria for localization of disease as described below.

Multicenter Trial Patients. Seven hospitals from different geographical locations utilizing various camera/computer systems participated in the multicenter trial evaluation (Table 1). Type A sites consisted of institutions imaging with Siemens camera/computer equipment and Type B sites consisted of institutions imaging with General Electric camera/computer equipment. A total of 161 patients who underwent rest/stress ^{99m}Tc-sestamibi SPECT imaging were included in the study population. The patients consisted of 2 groups: (1) 37 consecutive patients who were considered normal by having a <5% likelihood of CAD and (2) 124 consecutive patients who underwent coronary angiography (Table 2). One hundred and two of 124 patients had ≥50% coronary luminal diameter narrowing involving one (n = 43), two (n = 35), or three (n = 24) coronary arteries. The remaining 22 patients had <50% luminal diameter narrowing. Additionally, patients were categorized according to ≥70% as the criteria for significant coronary stenosis.

Patients for Establishing Criteria for Localization of Disease. An additional population consisting of 45 patients (39 male and 6 female) were used to establish the optimal criteria for localization of CAD in individual coronary arteries. In this group, there were 19 with LAD, 15 with LCX and 11 with RCA disease. None of these patients had prior myocardial infarction.

Exercise and Imaging Procedure

All patients were studied using the previously reported optimal image acquisition and processing protocols (*24,25*). Briefly, the protocol involved a same-day rest/stress imaging approach. The ^{99m}Tc sestamibi doses for a 70 kg patient were 8 mCi for the rest and 22 mCi for the exercise study. For heavier patients, doses were adjusted upward by 0.11 mCi/kg for the resting and 0.31 mCi/kg for the stress study. Patients were instructed to drink 8 oz of whole milk or ingest a light, fatty meal 15 min before imaging to promote tracer clearance from the gallbladder.

Rest images were acquired 1 hr after injection to allow for clearance from the hepatobiliary system. After an interval of 3–4 hr from the time of rest injection, the patient exercised on the treadmill according to the standard Bruce protocol. Exercise was symptom limited (moderately severe anginal pain, severe dyspnea or severe fatigue), unless one of the following developed: ≥4 mm ST segment depression, malignant arrhythmia or exercise hypotension (greater than 10 mm Hg drop between exercise stages). If the patient had left ventricular hypertrophy or was taking digoxin, the ST segment response (>4 mm depression) did not constitute reason for termination. Exercise continued for at least 1 min after injection and imaging was begun 30 min after exercise. Patients who achieved <85% of the maximal predicted heart rate and did not develop angina or ischemic ST depression were excluded, as were females with bra size of C-cup or greater and patients with left bundle-branch block. Studies in which the patients moved, identified by viewing the cine display of the raw projection data, were also excluded as were patients with prior coronary bypass surgery or precutaneous transluminal coronary angioplasty.

Acquisition Protocol

The image acquisition parameters for all rest-stress studies were a 20% symmetric energy window over the 140-keV photopeak, a high-resolution collimator and a circular 180° orbit using 64 projections from 45° right anterior oblique to 45° left posterior oblique in the supine position. All data was stored in 64 × 64 matrices. Acquisition time per projection was 25 sec for the resting study and 20 sec for the exercise study.

Computer Processing and Analysis

Tomographic Reconstruction. Each of the projections was corrected for nonuniformity with a flood source image containing

TABLE 2
Patient Populations

								Stenosis criteria (≥50%)				Stenosis criteria (≥70%)			
	Total	Mean Age	Range	M	F	LL	%MI	NCA	SV	DV	TV	NCA	SV	DV	TV
Type A	75	56.0	33–90	63	12	12	20	9	24	18	12	15	28	11	10
Type B	86	55.0	18–85	59	27	25	17	13	19	17	12	25	20	8	7
Combined	161	55.5	18–90	122	39	37	19	22	43	35	24	40	48	19	17

NCA = Normal coronary arteries; % MI = % myocardial infarction; M = males; F = females; SV = single-vessel disease; DV = double-vessel disease; TV = triple-vessel disease; LL = low likelihood normal patients; Type A = Siemens sites; and Type B = General Electric sites.

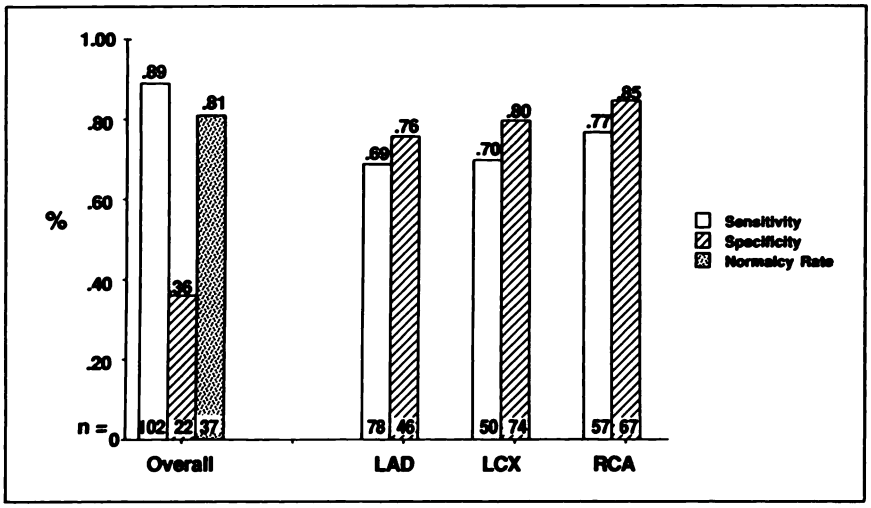

FIGURE 1. Combined results (Type A + Type B) for the overall sensitivity (CAD population), specificity (NCA population), normalcy rate (low likelihood population) and sensitivity and specificity for localization of disease in individual coronary arteries.

30 million counts and the mechanical center of rotation was determined in order to align the projection data with respect to the reconstruction matrix. Acquired projections of the rest and exercise studies were automatically corrected for radioactive decay from the start of image acquisition and prefiltered using a two-dimensional Butterworth filter. For the Type A systems, the filter parameters for stress imaging were: critical frequency of 66% Nyquist, order 2.5, and for rest images were: critical frequency of 50% Nyquist, order 5. For the type B systems the filter parameters for stress were: critical frequency of 0.52 cycles/cm, power 5, and for rest images were: critical frequency of 0.4 cycles/cm, power 10. The transaxial tomograms were reconstructed into image slices one pixel thick (6.4 mm) using a ramp filter and filtered backprojection. Short-axis tomograms of the entire left ventricle were extracted from the reconstructed transaxial tomograms by performing coordinate transformation re-orientation with appropriate interpolation. No attenuation or scatter correction was used. Adjacent 6.4 mm slices were then combined two at a time (staggered summation) to produce a new set of tomograms, each representing a physical thickness of 12.8 mm.

Quantitative Analysis. Processing parameters for Type A systems were automatically selected by the computer and then verified by an operator. For Type B systems, the parameters were selected manually. In either case, the following processing parameters were determined: the apical and basal short-axis slices, the central axis of the ventricular chamber, and a limiting radius (from the LV center) for myocardial count search.

Maximum count circumferential profiles were then generated for all short-axis tomograms, including the base. A hybrid search algorithm was employed to extract the three-dimensional tracer distribution by sampling perpendicularly to the myocardial wall. The apical slices were sampled in a spherical manner, while the remainder of the myocardium was sampled using a cylindrical search (*24*). Maximum count circumferential profiles were automatically generated from all short-axis slices using this two-part sampling scheme. The stress and rest profiles were normalized to the most normal wall of the entire patient's stress study prior to comparison to the normal limits (*27*).

Several quantitative polar maps were created from the profile data. Separate polar maps were generated for the rest and stress myocardial perfusion distributions and for the severity and reversibility of defects (*24,25*). Defect extent polar maps for rest and stress were generated after comparing the patients profiles to gender-matched normal limits. In this multicenter trial study, only

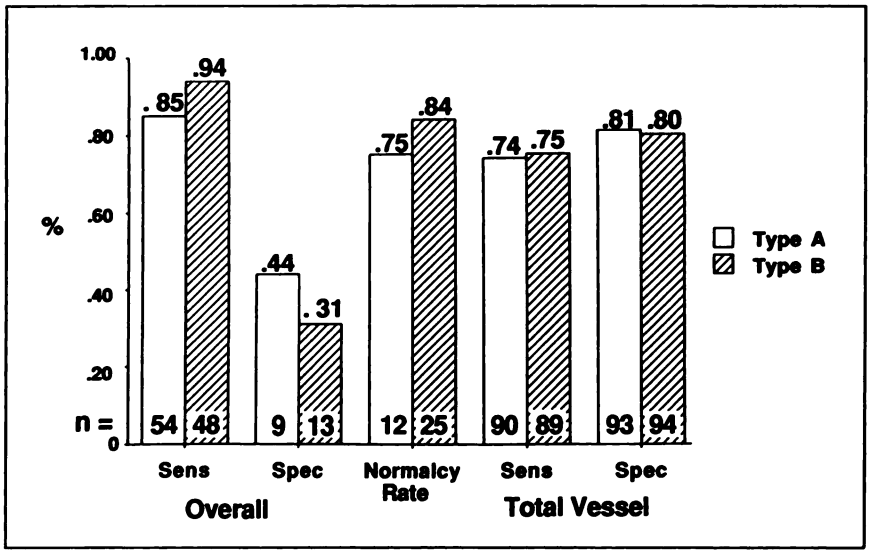

FIGURE 2. Overall sensitivity, specificity, normalcy rates, and total vessel sensitivity and specificity with respect to Type A and Type B sites. p = ns between Type A and Type B sites.

TABLE 3
Sensitivity Based on Number of Diseased Vessels

	Stenosis Criteria					
	≥50%			≥70%		
	SV	DV	TV	SV	DV	TV
Type A	17/19 (.89)	17/17 (1.0)	12/12 (1.0)	19/20 (.95)	8/8 (1.0)	7/7 (1.0)
Type B	19/24 (.79)	15/18 (.83)	11/12 (.92)	24/28 (.86)	9/11 (.82)	10/10 (1.0)
Combined	36/43 (.84)	32/35 (.91)	23/24 (.96)	43/48 (.90)	17/19 (.90)	17/17 (1.0)

SV = single-vessel disease; DV = double-vessel disease; TV = triple-vessel disease; Type A = Siemens sites; and Type B = General Electric sites.

the stress defect extent polar maps were used for detection and localization of CAD.

Development of Criteria for Detection of Disease in the Three Coronary Territories

For localization of CAD, the polar maps were divided into three (LAD, LCX and RCA) territories according to the approach previously described for ^{201}Tl (*18*). In each of the three coronary vascular territories, the total percentage of circumferential profile points that fell below the normal limits was determined in the group of 45 patients with single-vessel coronary disease. With the use of receiver operating characteristic curve analysis, various criteria for perfusion abnormality were assessed to determine those that provided the optimal true-positive versus false-positive trade-off for identifying disease in each of the three coronary arteries.

Analysis of Multicenter Trial Data

Patient data were acquired and reconstructed at each of the sites. Tomographic image files, cath report, ECG report, visual interpretation, patient demographic data and history were then sent to either Cedars–Sinai or Emory University for quantitative analysis. The final results were then tabulated for this study. Correlation of visual to quantitative analysis was performed by comparing the visual scores derived by consensus of each of the three vascular territories to the quantitative result of the corresponding territory on the polar map. Consensus was reached by two experienced observers using a 5-point scoring system (0 = normal; 1 = equivocal; 2 = moderate; 3 = severe reduction of radioisotope uptake; and 4 = absence of detectable tracer in a segment). The observers were unaware of the clinical history, stress testing results and results of coronary angiography.

Statistical Analysis

For overall detection of disease, sensitivity was defined as the proportion of patients with significant coronary disease, ≥50% in one or more coronary vessel, demonstrating an abnormal ^{99m}Tc sestamibi quantitative defect extent polar map. Specificity was defined by the proportion of patients without significant CAD demonstrating a normal ^{99m}Tc-sestamibi quantitative defect extent polar map. The term "normalcy rate" was defined as the proportion of patients with a low likelihood of CAD (<50%) who had a normal quantitative polar map. We used this group to approximate the true specificity of the test which may be greatly different from the observed specificity in normal coronary arteriogram patients due to post-test referral bias (*30–32*). For detection of disease in individual coronary arteries, only the catheterized patients were evaluated. Vessel sensitivity was defined as the proportion of vessels with ≥50% or ≥70% stenosis having an abnormality in the corresponding territory of the ^{99m}Tc sestamibi quantitative defect extent polar map. Vessel specificity was defined as the proportion of vessels with <50% or <70% stenosis having a normal polar map in the corresponding territory. Sensitivities, specificities, and normalcy rates were compared in males and females as well as MI and non-MI subgroups using either the chi-squared test or the Fisher's exact test and were tested at the alpha-0.05 level of significance. Computations were made using BMDP (Berkeley, CA) and SAS (Cary, NC) statistical software (*33,34*).

RESULTS

Overall Accuracy for Detection of CAD and Normalcy Rates

The results for overall accuracy were a sensitivity of 89%, specificity of 36% and a normalcy rate of 81% (Fig. 1). This data was further categorized according to the type of camera/computer system and these results are shown in Figure 2. In the comparison of type A and type B sites the overall sensitivities were 85% versus 94%, overall specificities were 44% versus 31%, and normalcy rates were 75% versus 84%. These data were derived based on defin-

TABLE 4
Overall Detection of Disease

	Stenosis Criteria					
	MI	Non-MI	≥50%	≥70%	Male	Female
Sensitivity	0.90 (27/30)	0.89 (64/72)	0.89 (91/102)	0.91 (75/82)	0.89 (76/85)	0.94 (16/17)
Specificity	—	—	0.36 (8/22)	0.30 (12/40)	0.44 (4/9)	0.31 (4/13)
Normalcy Rate	—	—	—	—	0.86 (24/28)	0.67 (6/9)

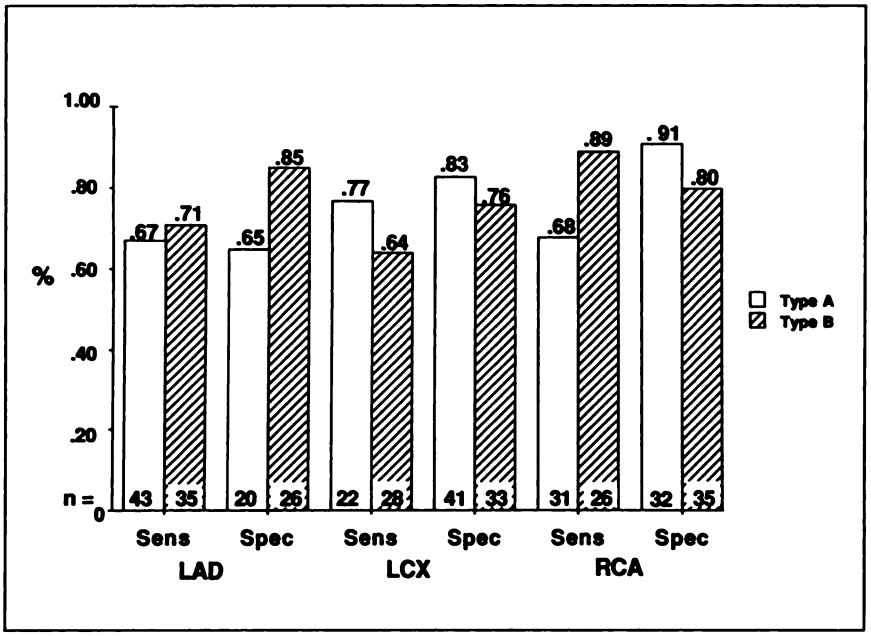

FIGURE 3. Sensitivity and specificity for localization of CAD with respect to Type A and Type B sites. p = ns between Type A and Type B sites.

ing CAD as at least one vessel having a ≥50% stenosis based on coronary angiography. As shown, no significant difference was noted between the two different types of camera/computer sites in this regard. The sensitivity for overall detection of disease increased with the number of diseased vessels; 84% in single-vessel disease, 91% in double-vessel disease and 96% in triple-vessel disease when the stenosis criteria of ≥50% was used (Table 3).

Using a criteria of ≥50% stenosis in the 72 patients without prior myocardial infarction, sensitivity for detection of disease was 89%, which was similar to that observed in the 30 patients with prior myocardial infarction (Table 4). When the criteria of ≥70% was used to define significant CAD, 82 patients were categorized as having disease (40 patients had <70% stenosis). Using this criterion, the sensitivity and specificity were 91% and 30% respectively which were not significantly different from those observed with the ≥50% criteria (Table 4). When the ≥70% criteria was used to determine sensitivity for overall detection of disease based on the number of diseased vessels, a sensitivity of 90% for single-vessel disease, 90% for double-vessel disease, and 100% for triple-vessel disease was obtained, which was similar to the results obtained when the ≥50% criteria was used (Table 3). The sensitivity, specificity, and normalcy rate for males and females separately are shown in Table 4. No significant differences were noted between the two genders, even though the normalcy rate appeared to be higher in the male (86%) versus the female (67%) population.

Criteria for Localization of Disease

Receiver operating characteristic curve analysis performed on the data derived from the 45 patients with single-vessel CAD determined the following optimal criterion for abnormality: ≥10% of the pixels were required to be abnormal in the left anterior descending and left circumflex coronary artery territories and ≥12% in the right coronary/posterior descending artery territory in order for it to be a quantitatively significant defect. When the criteria were applied, the true-positive and true-negative rates obtained in these 45 patients were 90% (17/19) and 96% (25/26) respectively for the left anterior descending, 82% (9/11) and 88% (30/34) for the left circumflex and 87% (13/15) and 93% (28/30) for the right coronary/posterior descending coronary artery territory.

Identification of Individual Diseased Coronary Arteries

The sensitivity and specificity for the localization of CAD is shown in Figures 1–3. Sensitivity and specificity were respectively 69% and 76% for LAD, 70% and 80% for LCX, and 77% and 85% for RCA (Figure 1). As shown in Figures 2 and 3, no significant differences were noted between type A and type B centers with respect to sensitivity and specificity for detection of disease in individual coronary arteries. The sensitivity and specificity were further broken down according to ≥50% and ≥70% stenosis and are shown in Figures 4 and 5. As expected, there was a trend for a higher sensitivity with slightly lower specificities when the less stringent ≥70% stenosis criteria was employed.

The sensitivity for localization of CAD in the MI versus non-MI patients for the LAD was 81% (17/21) versus 65% (37/57), the LCX was 71% (12/17) versus 70% (23/33), and the RCA was 77% (17/22) versus 77% (27/35). The specificity for localization of CAD in the MI versus non-MI patients for the LAD was 89% (8/9) versus 67% (10/15), the LCX was 85% (11/13) versus 87% (34/39), and the RCA was 75% (6/8) versus 70% (26/37). There were no significant differences between these two groups of patients.

Correct Identification of the Extent of Disease

Table 5 shows the relationship between quantitative perfusion data and angiographic results with respect to cor-

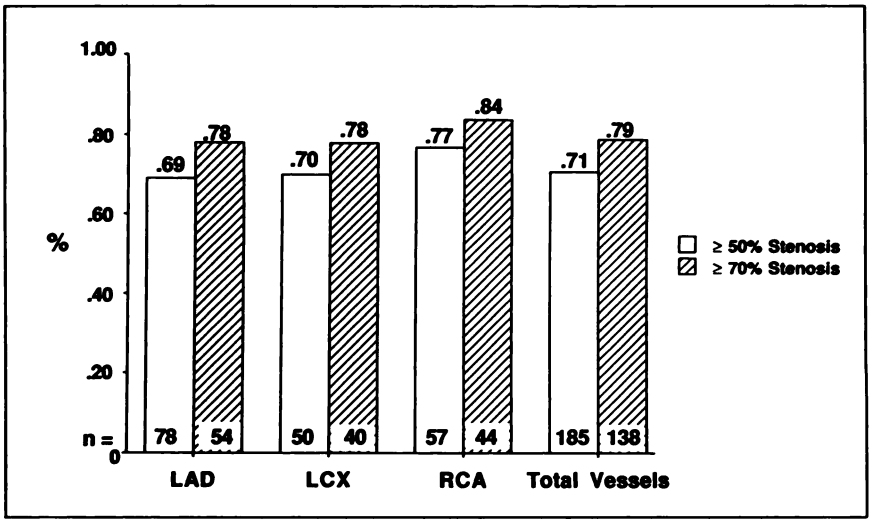

FIGURE 4. Sensitivity for localization of CAD based on a stenosis size criteria of ≥50% and ≥70%. p = ns between ≥50% and ≥70%.

rectly identifying the extent of coronary disease (total number of diseased vessels) in patients using a ≥50% stenosis criteria. Of 43 patients with single-vessel disease, the quantitative ^{99m}Tc-sestamibi method correctly classified 21 (49%) as single-vessel disease, 14 as double-vessel disease, 1 as triple-vessel disease, and 7 as not having CAD. Of the 35 patients with double-vessel disease by angiography, 15 (43%) were correctly identified as having double-vessel disease by quantitative ^{99m}Tc-sestamibi method. Of the 24 patients with triple-vessel disease by angiography, nine (38%) were correctly identified as having triple-vessel disease by quantitative ^{99m}Tc-sestamibi method. Of the total of 59 patients with multivessel disease, ^{99m}Tc-sestamibi correctly identified 35 (59%) as having multivessel disease, 20 (34%) as having single-vessel disease, and four (7%) as having normal coronaries. Additionally, there was only one patient with documented triple-vessel disease by catheterization that had a normal quantitative SPECT study and there were no patients with normal coronary arteries who were falsely identified as having triple-vessel disease by the quantitative technique.

Visual Versus Quantitative Analysis

The results comparing visual versus quantitative findings for overall detection and localization of perfusion abnormalities are shown in Table 6. The quantitative results correlated with those of visual interpretation, with an agreement of 89% for overall identification of disease. Furthermore, the two methods correlated for the identification of defects in the territories of different coronary arteries; 88% for LAD, 83% for LCX and 80% for the RCA.

DISCUSSION

Accurate visual interpretation of myocardial perfusion SPECT tomograms requires knowledge of the normal patterns of myocardial count distribution in males and females, which can only be achieved through an extensive review of normal and abnormal studies. In addition, visual analysis only offers a subjective indication as to the extent, severity and reversibility of a defect, and is not optimal for comparison of serial studies.

The quantitative method in this study uses normal male

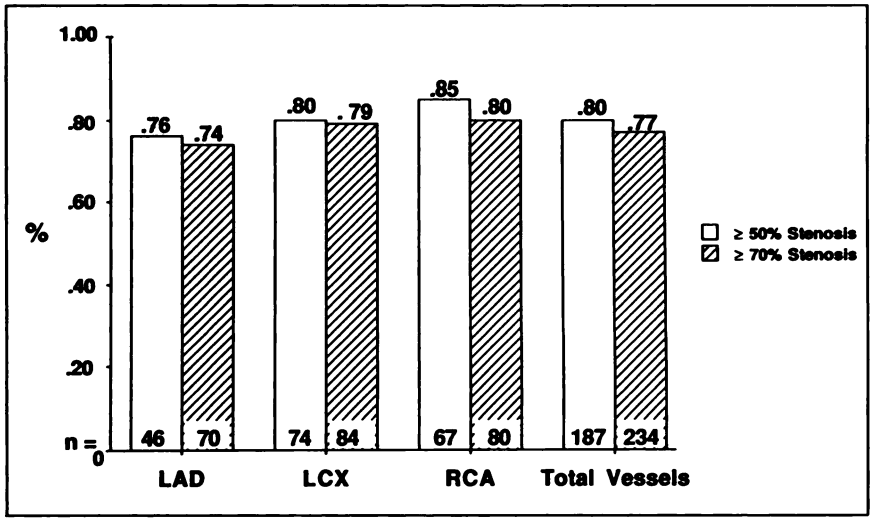

FIGURE 5. Specificity for localization of CAD based on a stenosis size criteria of <50% and <70%. p = ns between <50% and <70%.

TABLE 5
Accuracy for Correct Vessel Detection (≥50% Stenosis)

	Quantitative ^{99m}Tc Sestamibi Results			
	NCA	1-Vessel Disease	2-Vessel Disease	3-Vessel Disease
Coronary Angiography Results				
NCA	8	6	8	0
1-Vessel Disease	7	21	14	1
2-Vessel Disease	3	14	15	3
3-Vessel Disease	1	6	8	9

and female myocardial distribution data bases and offers an objective assessment of a patient's myocardial perfusion. Integration of the quantitative method with visual interpretation can accelerate the development of the necessary skills required for the accurate interpretation of these studies. Importantly, quantitative values derived from the algorithm for the extent of perfusion defects can be used to objectively stage sequential myocardial perfusion studies.

Prior to widespread clinical application of the method, several important issues needed to be addressed:

1. Would the accuracy produced in the pilot study (*27*) also be obtained in a larger population?
2. Would similar accuracy be obtained when different camera/computer systems are utilized?
3. Would the gender specific normal limits also apply to populations from different institutions?
4. In a larger population, what is the accuracy in patients with and without prior myocardial infarction? This study was undertaken to address these issues.

Imaging Method

Same-day rest/stress imaging protocol as opposed to stress/rest protocol was utilized in this study for several reasons:

1. This protocol allows better assessment of defect reversibility as shown by Taillefer et al. (*4–6*).
2. The entire study can be completed in 5–6 hr, in fact, although not a part of this investigation, it is estimated that by increasing the stress dose, the total time of the study can be reduced to 2 hr with no further compromise on defect contrast.
3. The high dose used for stress images results in high-quality images and allows for first-pass studies and multiple gated tomography, which may be useful for assessing ejection fraction (*35–37*), wall motion, wall thickening (*38–41*) and for ruling out image artifacts.

For processing these studies, previously optimized filters defined separately for the rest and exercise studies were used in order to generate tomograms of comparable image quality from images of different count density (*24*). Since various computer manufacturers define filters differently, optimal filters for each system were determined separately.

The quantitative method utilized for this analysis (*24,27*) included significant enhancements over our previous ^{201}Tl quantitative techniques (*14,17*). The short-axis tomograms and processing parameters (cavity center and radius of search) are selected automatically. This feature results in increased objectivity and reproducibility of the analysis. An improved method for apical sampling is employed where the apical portion of the short-axis slices are sampled using a spherical search and the remainder of the myocardium is sampled using cylindrical search. Both distance- and volume-weighted polar maps were created, thus offering an improved technique for visualizing the true size and location of the defect. A more comprehensive technique for normalization is employed which involves sampling eight sectors rather than four (*17*) for determining the most normal sector. The increased sample size allows for a more accurate definition of the normal territory to be used for the normalization process. Varying standard deviations for the five myocardial regions (apex, anterior, lateral, inferior, and septum) are used to establish the threshold for defect detection. Previous approaches utilized a single standard deviation (*17*) or a range approach (*18*) for the threshold. The varying standard deviations potentially offer a better definition and localization of the defect than the previous approaches.

The results reported here are based on comparing both coronary angiographic findings (Figures 1–5, Tables 3–5) and expert visual interpretation (Table 6).

TABLE 6
% Agreement Between Quantitative and Visual Analysis for Identification of Disease in Patients and in Individual Vessels

	Overall	LAD	LCX	RCA
True-Positive	0.94 (98/104)	0.87 (54/62)	0.77 (41/53)	0.78 (50/64)
True-Negative	0.60 (12/20)	0.89 (55/62)	0.87 (62/71)	0.82 (49/60)
Combined agreement	0.89 (110/124)	0.88 (109/124)	0.83 (103/124)	0.80 (99/124)

Overall Accuracy for Detection of CAD and Normalcy Rates

The overall sensitivity for detection of disease in the total population, MI versus non-MI, male versus female, and ≥50% versus ≥70% stenosis were all similar, ranging between 89% and 94% (Fig. 1 and Table 4). In addition, the comparison between sensitivity results derived from the Type A and Type B sites was also similar, 85% versus 94% respectively (Fig. 2).

The overall specificity in the normal coronary artery patients and normalcy rate in the low-likelihood patients was 36% (8/22) and 81% (30/37) respectively (Fig. 1). Most likely, the predominant reason for the reduced specificity is the referral bias in this population. The normalcy rate offers another measure related to specificity which utilizes patients with a <5% likelihood of having CAD to determine the performance of the test in a normal population. The normalcy rate in the female population was considerably lower than the male: 67% versus 86% (Table 4). This lower specificity in the female population was most likely due to variable breast attenuation in females. Two of the three false-positive low-likelihood females had localized anterior perfusion defects, which were visually interpreted as breast attenuation artifact. Attenuation artifacts which can be visually identified explain most of the errors in the normalcy rate. Of the seven false-positive low-likelihood CAD patients, only two were also read abnormal by visual interpretation. Additionally, in the patients who were found to have normal coronary arteries by angiography, visual analysis corroborated the quantitative findings in ten out of 14 of these false-positive patients.

The accuracy for localization of disease in the MI versus non-MI populations showed no significant difference between the two populations. The specificity in the LAD distribution did show a trend for higher specificity, 89% for MI versus 67% for non-MI, but this was probably due to the small sample size in this population.

It should be noted that comparative accuracy between genders (Table 4) was determined with an unequal number of patients (male = 122, female = 39). While analyzing an equal number of female patients would have been preferred, it would have increased the study length considerably since the female patients only represented approximately 25% of the patient referral population. The female sample size was similar to our previous ^{201}Tl multicenter trial validation (*20*) which demonstrated similar results in a comparable gender distribution (male = 209, female = 33).

Development of Criteria for Detection of Disease in the Three Coronary Territories

The criteria for localization of disease in the previous paper (*27*) utilized the ^{201}Tl thresholds (LAD and LCX: 12% and RCA: 8%) for establishing the accuracy for localizing CAD. This study involved a further investigation to establish criteria specific for ^{99m}Tc-sestamibi myocardial perfusion. While the investigation demonstrated no significant difference in the location of the coronary artery polar map boundaries, the criteria were found to be slightly different, being 10% for the LAD and LCX and 12% for the RCA.

Identification of Individual Diseased Coronary Arteries

There was no significant difference between the two computer systems in sensitivity or specificity for localization of disease. Also, as expected, there was a trend for a slightly higher specificity and lower sensitivity in each of the coronary arteries when the ≥50% stenosis criteria was used, compared to the ≥70% stenosis criteria (Fig. 4 and 5).

The lowest sensitivity was experienced in the left anterior descending (69%) and left circumflex (70%) territory. This lower sensitivity could be attributed to the degree of stenosis in these vessels. Of the 24 false-negative LAD and 15 false-negative LCX quantitative results, half of these vessels (13 LAD and 7 LCX) were in vessels with stenosis size between 50%–60%.

Correct Identification of the Extent of Disease

Table 5 demonstrates that the accuracy for correctly identifying diseased vessels was less than 50% for single-, double-, or triple-vessel disease. Similar results have been reported with ^{201}Tl SPECT. One reason for this reduced accuracy may be that not all diseased vessels develop a relative flow reduction during peak exercise. Patients with multivessel disease who undergo stress may have their exercise capacity limited by the development of ischemia in the most severely diseased zone. These patients may only demonstrate a reduction in flow to their most severely stenosed vessel. Another factor contributing to the difficulty in quantitatively localizing disease is related to the fixed territories employed in the analysis. An abnormal left anterior descending coronary artery producing a perfusion defect often extends out of the LAD territory on the quantitative polar map into an adjacent territory. Thus, a single-vessel disease study is incorrectly called double-vessel disease by the quantitative technique.

Visual Versus Quantitative Analysis

Table 6 demonstrates that a high degree of correlation exists between expert visual interpretation and the quantitative results for detection and localization of perfusion abnormalities. In practice, clinical interpretation of tomographic studies should involve integrating both visual and quantitative results. The benefit of integrating the results is demonstrated in the improvement obtained in the overall quantitative true negative rate of 60% (12/20) if the visual results are also considered. Of the eight false-positive patients three were females and five were males. Two of the female patients had breast artifact which were read normal by visual interpretation. In the male population, four of the five patients had equivocal visual scores and were found to have a ≥50% stenosis in their corresponding coronary artery.

Comparison Versus Thallium-201

Thallium-201 has been the primary agent of choice for myocardial perfusion imaging over the past 17 years.

Therefore, a comparison of the multicenter trial quantitative ^{201}Tl results (*20*) with these ^{99m}Tc-sestamibi results is included in this section. This comparison must be viewed with some caution since the ^{201}Tl multicenter trial population contained more disease than the current ^{99m}Tc-sestamibi population. The composition of disease in the ^{201}Tl versus ^{99m}Tc-sestamibi groups included 33% (64/196) versus 42% (43/102) with single-vessel disease, 37% (72/196) versus 34% (35/102) with double-vessel disease, and 31% (60/196) versus 24% (24/102) with triple-vessel disease. The overall detection of disease was 89% (91/102) in the ^{99m}Tc-sestamibi multicenter trial population. This was similar to the ^{201}Tl multicenter trial results which showed overall sensitivity of 94% (184/196).

The overall specificity in the normal coronary artery patients and normalcy rate in the low-likelihood patients was 36% (8/22) and 81% (30/37) respectively. These values were not significantly different statistically to the previous ^{201}Tl multicenter trial results: 44% (20/46) and 82% (62/76) respectively.

Technetium-99m-sestamibi had a higher specificity but lower sensitivity for localization of disease than the previous ^{201}Tl multicenter trial results. The sensitivities for ^{201}Tl versus ^{99m}Tc sestamibi were 78% (115/148) versus 69% (54/78) for LAD, 68% (66/97) versus 70% (35/50) for LCX, and 84% (118/141) versus 77% (44/57) for RCA. The specificities were 63% (59/94) versus 76% (35/46) for LAD, 68% (98/145) versus 80% (59/74) for LCX, and 62% (63/101) versus 85% (57/67) for RCA. Overall, there appears to be a trend for lower sensitivity and higher specificity with ^{99m}Tc-sestamibi. This is due in part to the greater prevalence of disease in the ^{201}Tl multicenter trial population compared to the ^{99m}Tc-sestamibi population. However, one cannot rule out the possibility that the ^{99m}Tc-sestamibi perfusion agent produces defects which are smaller and less severe than the ^{201}Tl images. Narahara et al. (*42*) recently reported results demonstrating that defect size on stress images with ^{99m}Tc sestamibi is reduced and less severe than with ^{201}Tl imaging. However, when the data in this study was analyzed according to the ability to correctly identify diseased vessels, there was no trend for the underestimation of disease with ^{99m}Tc-sestamibi (Table 5).

LIMITATIONS

As was previously mentioned, localization of CAD was determined using fixed coronary territories defined on the polar maps. A more accurate method for localization of disease would involve incorporating artificial intelligence rules similar to those employed by experts at the time of visual interpretation. The problem associated with interpreting a single-vessel disease as a double-vessel due to extension of a defect into an adjacent vascular territory probably could be correctly interpreted by using a rule-based expert system. Rules which consider defect size, shape, and extension would potentially offer a better opportunity to correctly localize disease to the proper territory. A program incorporating these artificial intelligence rules is being developed (*43*) and should improve the method's accuracy when using coronary angiography as the gold standard. Similar rules could be helpful in identifying attenuation artifacts. The expert visual reader incorporates location assessment of the defects and defect reversibility in calling abnormality, although these aspects are not yet incorporated in the present quantitative program.

The program's accuracy in female patients is reduced due to the variable breast attenuation, which is unaccounted for in this version of the program. For this reason the program is currently limited to analyzing females with a breast cup size of B or less. The solution for breast and diaphragmatic attenuation is to apply a correction method for scatter and variable attenuation to the patients study prior to quantitation. This problem is being addressed by several investigators (*44–47*) and preliminary animal work employing their methodology appears promising.

CONCLUSION

These multicenter trial results have demonstrated that this new objective quantitative analysis method for same-day rest-stress ^{99m}Tc-sestamibi SPECT utilizing gender specific normal limits is clinically applicable for the accurate detection and localization of CAD in institutions other than our own. The accuracy obtained was similar for the two types of camera/computer equipment used in this study. Finally, in addition to being accurate based on coronary angiography, the program also correlates well with expert visual interpretation.

ACKNOWLEDGMENTS

The authors appreciate the significant contribution made by all of the participants (and centers) in this multicenter trial. The authors also thank Mila Abarrientos and Fan-Ping Wang, MD for technical support.

This study was supported in part by grants RO1-HL41628 and RO1-HL42052 from the National Institute of Health, Bethesda, MD, by a grant from the American Heart Association, Greater Los Angeles Affiliate, as well as by a grant from E.I. du Pont de Nemours & Co., North Billerica, MA.

This work was presented in part at the 39th Annual Scientific Session of the Society of Nuclear Medicine, Los Angeles, CA June 1992.

REFERENCES

1. Leppo JA, Meerdink DA. Comparison of the myocardial uptake of a technetium-labeled isonitrile analogue and thallium. *Circ Res* 1989;65:632–639.
2. Okada RD, Glover D, Gaffney T, et al. Myocardial kinetics of technetium-99m-hexakis-2-methoxy-2-methylpropyl-isonitrile. *Circulation* 1988;77:491–449.
3. Kahn JK, Henderson EB, Akers MS, et al. Gated and ungated tomographic perfusion imaging with technetium-99m RP30A: comparison with ^{201}Tl tomography in coronary artery disease [Abstract]. *J Am Coll Cardiol* 1988; 11:32A.
4. Taillefer R, Laflamme L, Dupras G, et al. Myocardial perfusion imaging with ^{99m}Tc-methoxy-isobutyl-isonitrile (MIBI): comparison of short and long time intervals between rest and stress injections. *Eur J Nucl Med* 1988;13:515–522.
5. Taillefer R, Gagnon A, Laflamme L, et al. Same day injections of ^{99m}Tc methoxy isobutyl isonitrile (hexamibi) for myocardial tomographic imaging:

comparison between rest-stress and stress-rest injection sequences. *Eur J Nucl Med* 1989;15:113–117.
6. Taillefer R. Technetium-99m sestamibi myocardial imaging: same-day rest-stress studies and dipyridamole. *Am J Cardiol* 1990;66:80E–90E.
7. Buell U, Dupont F, Uebis R, et al. Technetium-99m-methoxy-isobutyl-isonitrile SPECT to evaluate a perfusion index from regional myocardial uptake after exercise and at rest: results of a four hour protocol in patients with coronary heart disease and in controls. *Nucl Med Commun* 1990;11: 77–94.
8. Garcia EV, Maddahi J, Berman DS, et al. Space-time quantitation of ^{201}Tl myocardial scintigraphy. *J Nucl Med* 1981;22:309–317.
9. Maddahi J, Garcia EV, Berman DS, et al. Improved noninvasive assessment of CAD by quantitative analysis of regional stress myocardial distribution and washout of thallium-201. *Circulation* 1981;64:924–935.
10. Watson DD, Campbell NP, Read EK, et al. Spatial and temporal quantitation of planar thallium myocardial images. *J Nucl Med* 1981;22:577–584.
11. Berger BC, Watson DD, Taylor GJ, et al. Quantitative ^{201}Tl exercise scintigraphy for detection of coronary artery disease. *J Nucl Med* 1981;22:585.
12. Massie B, Hollenberg M, Wisneski JA, et al. Scintigraphic quantitation of myocardial ischemia: a new approach. *Circulation* 1983;68:747.
13. Tamaki N, Yonekura Y, Mukai T, et al. Stress ^{201}Tl transaxial emission computed tomography: quantitative versus qualitative analysis for evaluation of coronary artery disease. *J Am Coll Cardiol* 1984;4(6):1213.
14. Garcia E, Van Train K, Maddahi J, et al. Quantification of rotational thallium-201 myocardial tomography. *J Nucl Med* 1985;26:17–26.
15. Van Train K, Berman DS, Garcia E, et al. Quantitative analysis of stress ^{201}Tl myocardial scintigrams: a multicenter trial validation utilizing standard normal limits. *J Nucl Med* 1986;27:17–25.
16. Kaul S, Chesler D, Boucher C, Okada R. Quantitative aspects of myocardial perfusion imaging. *Semin Nucl Med* 1987;17:131.
17. DePasquale EE, Nody AC, DePuey EG, et al. Quantitative rotational thallium-201 tomography for identifying and localizing coronary artery disease. *Circulation* 1988;77:316–327.
18. Maddahi J, Van Train KF, Prigent F, et al. Quantitative single photon emission computerized thallium-201 tomography for the evaluation of coronary artery disease: optimization and prospective validation of a new technique. *J Am Coll Cardiol* 1989;14:1689–1699.
19. Iskandrian AS, Heo J, Kong B, Lyons E. Effect of exercise level on the ability of thallium-201 tomographic imaging in detecting coronary artery disease: analysis of 461 patients. *J Am Coll Cardiol* 1989;14:1477–1486.
20. Van Train KF, Maddahi J, Berman DS, et al. Quantitative Analysis of tomographic stress thallium-201 myocardial scintigrams: a multicenter trial. *J Nucl Med* 1990;31:1168–1179.
21. Mahmerian JJ, Boyce TM, Goldberg RK, Cocanougher MK, Roberts R, Verani MS. Quantitative exercise thallium-201 single photon emission computed tomography for the enhanced diagnosis of ischemic heart disease. *J Am Coll Cardiol* 1990;15:318–329.
22. Kahn JK, McGhie I, Akers MS, et al. Quantitative rotational tomography with ^{201}Tl and ^{99m}Tc 2-methoxy-isobutyl-isonitrile: a direct comparison in normal individuals and patients with coronary artery disease. *Circulation* 1989;79:1282–1293.
23. Kiat H, Van Train KF, Maddahi J, et al. Development and prospective application of quantitative two-day stress-rest ^{99m}Tc methoxy isobutyl isonitrile SPECT for the diagnosis of coronary artery disease. *Am Heart J* 1990;120:1255–1266.
24. Garcia E, Cooke CD, Van Train KF, et al. Technical aspects of myocardial SPECT imaging with technetium-99m-sestamibi. *Am J Cardiol* 1990;66: 23E–31E.
25. Berman DS, Kiat H, Van Train KF, et al. Technetium-99m-sestamibi in the assessment of chronic coronary artery disease. *Semin Nucl Med* 1991;190–212.
26. Ezekiel A, Van Train KF, Berman DB, et al. Automatic determination of quantitation parameters from Tc-sestamibi myocardial tomograms. In: *Computers in cardiology*. New York, IEEE Computer Society; 1991:237–240.
27. Van Train KF, Areeda J, Garcia EV, et al. Quantitative same-day rest-stress Technetium-99m sestamibi SPECT: definition and validation of stress normal limits and criteria for abnormality. *J Nucl Med* 1993;34:1494–1502.
28. Diamond GA, Forrester JS. Analysis of probability as an aid in the clinical diagnosis of coronary artery disease. *N Engl J Med* 1979;300:1350–1358.
29. Diamond GA, Forrester JS, Hirsch M, et al. Application of conditional probability analysis to the clinical diagnosis of coronary artery disease. *J Clin Invest* 1980;65:1210–1221.
30. Rozanski A, Diamond GA, Berman DS, et al. The declining specificity of exercise radionuclide ventriculography. *N Engl J Med* 1983;309:518–522.
31. Maddahi J, Rozanski A, Becerra A, et al. Patients with a calculated very low likelihood of coronary artery disease: an alternative population of cardiac normals [Abstract]. *Circulation* 1982;66:II–62.
32. Rozanski A, Berman DS. The efficacy of cardiovascular nuclear medicine exercise studies. *Semin Nucl Med* 1987;17(2):104–120.
33. SAS Institute, Inc. *SAS user's guide: basics, Version 5 edition*. Cary, NC: SAS Institute Inc., 1985.
34. Dixon WJ, ed. *BMDP statistical software*. Berkeley: University of California Press, 1985.
35. Borges-Neto S, Coleman RE, Jones RH. Perfusion and function at rest and treadmill exercise using technetium-99m-sestamibi: comparison of one- and two-day protocols in normal volunteers. *J Nucl Med* 1990;31:1128–1132.
36. Borges-Neto S, Coleman E, Potts J, et al. Combined exercise radionuclide angiography and single photon emission computed tomography perfusion studies for assessment of coronary artery disease. *Semin Nucl Med* 1991; 21:223–229.
37. DePuey GE, Nichols K, Dobrinsky C. Left ventricular ejection fraction assessed from gated technetium-99m-sestamibi SPECT. *J Nucl Med* 1993; 34:1871–1876.
38. Marcassa C, Marzullo P, Parodi O, et al. A new method for noninvasive quantitation of segmental myocardial wall thickening using technetium-99m-2-methoxy-isobutyl-isonitrile scintigraphy—results in normal subjects. *J Nucl Med* 1990;31:173–177.
39. Ziffer J, La Pidus A, Alazraki N, et al. Predictive value of systolic wall thickening for myocardial viability assessed by ^{99m}Tc-sestamibi using a count based algorithm [Abstract]. *J Am Coll Cardiol* 1991;17:251A.
40. Faber TL, Akers MS, Peshock RM, et al. Three-dimensional motion and perfusion quantification in gated single-photon emission computed tomograms. *J Nucl Med* 1991;32:2311–2317.
41. Galt JR, Garcia EV, Robbins WL. Effects of myocardial wall thickness of SPECT quantification. *IEEE Trans Med Imaging* 1990;9:144–150.
42. Narahara KA, Villanueva-Meyer J, Thompson CJ, et al. Comparison of thallium-201 and technetium-99m hexakis 2-methoxyisobutyl isonitrile single-photon emission computed tomography for estimating the extent of myocardial ischemia and infarction in coronary artery disease. *Am J Cardiol* 1990;66:1438–1444.
43. Herbst MD, Garcia EV, Cooke CD, et al. Myocardial ischemia detection by expert system interpretation of ^{201}Tl tomograms. In: Johan Reiber, Hc & Ernst E. Van DerWall, eds. *Cardiovascular nuclear medicine and MRI*. London, England: Kluwer; 1992:77–88.
44. Galt J. Reconstruction of the absolute radionuclide distribution in a scattering medium from scintillation camera projections. Doctoral dissertation, Emory University, Atlanta, GA, 1988 (University Microfilms, Ann Arbor, MI).
45. Cullom SJ, Galt JR, Maddahi J. Scatter and attenuation correction of SPECT ^{99m}Tc sestamibi myocardial distributions: experimental validation of the effect on uniformity and contrast [Abstract]. *J Nucl Med* 1991;32: 1067.
46. Tung CH, Gullberg GT, Zeng GL, Christian PE, Datz FL, Morgan HT. Non-uniform attenuation correction using simultaneous transmission and emission converging tomography. In: *Nuclear Sci. Symp., IEEE Med. Imag.* 1991;2018–2022.
47. Bailey D, Hutton B, Walker P. Improved SPECT using simultaneous emission and transmission tomography. *J Nucl Med* 1987;28(5):844–851.